www.czasopisma.pan.pl PAN POLSKA AKADEMIA NAUK www.journals.pan.pl

A R C H I V E S O F M E T A L L U R G Y A N D M A T E R I A L S

Volume 56 2011 Issue 3

DOI: 10.2478/v10172-011-0073-1

M. O. SHABANI* , A. MAZAHERY**

PREDICTION OF MECHANICAL PROPERTIES OF CAST A356 ALLOY AS A FUNCTION OF MICROSTRUCTURE AND COOLING RATE

PRZEWIDYWANIE WŁAŚCIWOŚCI MECHANICZNYCH ODLEWNICZYCH STOPÓW ALUMINIUM A356 NA PODSTAWIE MIKROSTRUKTURY I SZYBKOŚCI CHŁODZENIA

In order to predict the mechanical properties of A356, a relatively new approach is presented in this paper using finite element technique which combines mechanical properties data in the form of experimental and simulated microstructures.

In this work, the comparison of this model's predictions with the ones in the literature is presented. It is revealed that predictions of this study are consistent with the other works and experimental measurements for A356 alloy. The results of this research were also used in order to form an analytical equations followed with solidification codes for SUT (Sharif University Technology) software.

Keywords: A356, mechanical, Dendrite arm spacing, Prediction

W celu prognozowania właściwości mechanicznych stopów A356, w pracy przedstawiono stosunkowo nowe podejście przy użyciu metody elementów skończonych, które łączy w sobie dane właściwości mechanicznych w formie badań eksperymentalnych i symulacji mikrostruktur.

W pracy przedstawiono porównanie przewidywań tego modelu z danymi literaturowymi i stwierdzono, że są one zgodne z innymi pracami i danymi eksperymentalnymi dla stopu A356. Wyniki tej pracy zostały również wykorzystywane do sformułowania równań analitycznych następnie użytych do programowania krzepnięcia w oprogramowaniu SUT (Sharif University of Technology).

1. Introduction

Cast aluminum–silicon alloys have an excellent combination of castability and mechanical properties, as well as good corrosion resistance and weldability [1-3]. Successful development of application of aluminum casting parts needs high strength and elongation. There are a number of effective parameters, which control mechanical properties of casting parts including grain size, dendrite arm spacing (DAS), size and distribution of secondary phases [4, 5]. The refinement of the microstructure leads to substantial improvement in mechanical properties. The secondary dendrite arm spacing controls the size and the distribution of porosity and intermetallic particles in the casting. Chemical composition, melting process, casting process and solidification rate determine the quality of the microstructure of aluminum parts. As DAS becomes smaller, porosity and second phase constituents are dispersed more finely and evenly which also enhances the mechanical properties [1, 6-11].

In 1966, Oldfield proposed that the heat source term, in the heat transfer equation could be represented by the function of nucleation rate and growth velocity of crystal grain, and he attempted to simulate the solidification microstructure of gray casting iron. Yet the micro simulation had been developed slowly, confined by the corresponding macro simulation during the followed years [12].

It is well established that under most conditions of solidification, the dendritic morphology is the dominant characteristic of the microstructure of off-eutectic alloys. Fine dendritic microstructures in castings, characterized by the dendrite arm spacing, are recognized to have superior mechanical properties than coarser ones, particularly when considering the tensile strength and ductility. Much more research has been devoted to the definition of the factors affecting the fineness of the dendritic structure.

* MATERIALS AND ENERGY RESEARCH CENTER (MERC), TEHRAN, IRAN

** DEPARTMENT OF MATERIALS ENGINEERING, TEHRAN UNIVERSITY, TEHRAN, IRAN

Numerous solidification studies have been reported with a view to characterize the primary and secondary dendrite arm spacing as a function of alloy solute concentration, tip growth rate and temperature gradient ahead of the macroscopic solidification front [13]. A eutectic constituent, comprising of aluminum-rich and silicon phases grows between the aluminum-rich dendritic networks. To describe the mechanical properties, we need parameters such as SDAS, yield stress (σ_y), ultimate tensile strength (UTS) and elongation percentage. In this paper, each of these length scales is discussed in detail. Analytical equations, generated for these length scales can be incorporated in the commercial software for prediction of microstructure in shape castings [14].

2. Experimental procedure

In this study, approximately 4.5 kg of A356 was charged into the crucible made from cast iron, heated up to above 720°C, and then the step casting was poured into the sand mould. The chemical analysis of the ingot used to make the step castings is presented in Table 1. Fifteen thermocouples were implemented to determine the experimental cooling rate. These thermocouples were located in 10, 40 and 75 mm from the side of each step. A side view and top view of the step castings are shown in Fig. 1. The casting was gated from the side of the riser. The casting was then sectioned and samples were extracted from steps 1 to 5. Transverse specimens were cut from the castings and prepared for tensile testing according to specifications of ASTM Standard B577M. In order to ensure the persuasion of results, five specimens were cut for each step and yield stress, ultimate tensile strengths and elongation percentage have been determined at each position.

For microstructural study, specimens were prepared by grinding through 80, 120, 200, 400, 800, 1000 and 2000 grit papers followed by polishing and etched with HF % 4. Then images from each sample were taken by optical microscope. The A356 alloy is a hypo-eutectic alloy consisting of primary α-Al dendrite and eutectic Si particles. These images were then analyzed using a commercial image-analysis software package. Quantitative metallography was conducted by a Clemex Image Analysis system (Clemex CIR^{TM} 3.5). The secondary dendrite arm spacing was obtained by a linear intercept method where the line is chosen to intersect a series of well-defined secondary dendrite arms. Most of the images were taken at the magnification of 50x, 100x and 200x. Then experimental SDAS was gained in different cooling rate and compared with simulated results.

TABLE 1

Chemical analysis of the ingot used for the step castings

Si	Fe	Cu	Mn	Mg	Zn	Ti	Cr	Ni	Pb	Sn
6.91	0.4	0.25	0.2	0.33	0.31	0.02	0.01	0.05	0.1	< 0.01

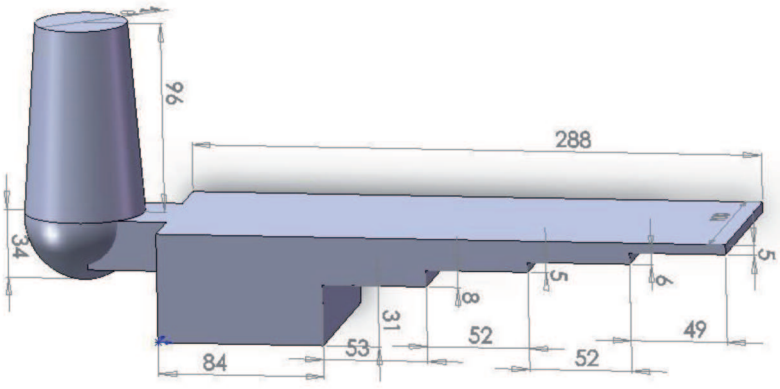

Fig. 1. Scale drawing for step castings

3. Prediction

A relation between microstructure and mechanical properties of A356 alloy is required for prediction of the mechanical properties. In this research, mechanical properties are considered as a function of secondary dendrite arm spacing.

3.1. secondary dendrite arm spacing

Numerous solidification studies have been developed with a view to characterize dendrite arm spacing under experimental circumstances involving solidification in the steady-state heat flow and those in the unsteady-state regime. The later case is of prime importance, since this class of heat flow regime encompasses the majority of industrial solidification processes. In this case, which is the focus of this article, secondary dendrite arm spacing (SDAS), is usually expressed as a function of local solidification time (t_f), Where M and K are constants [15]:

$$SDAS = K(Mt_f)^{1/3} \tag{1}$$

In this research, dendrite arm spacing was obtained in different casting temperature using image analysis technique. The variation of SDAS with cooling rate (R) is presented in Fig. 2.

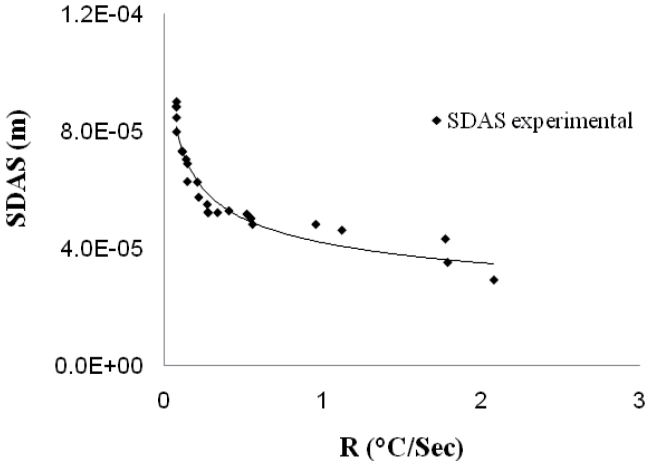

Fig. 2. Secondary dendrite arm spacing as a function of cooling rate for A356 alloy

Equation 3 can be extracted from this curve regarding $\Delta T = 60°C$:

$$t_f = \frac{60}{R} \tag{2}$$

$$SDAS = 10.4(t_f)^{1/3} \tag{3}$$

3.2. Mechanical properties

Variations of yield stress ($б_y$), ultimate tensile strength (UTS), maximum force (F_{max}) and elongation percentage (Δl) with secondary dendrite arm spacing are exhibited in Figure 3. These results are used to predict the mechanical properties and extract the following equations.

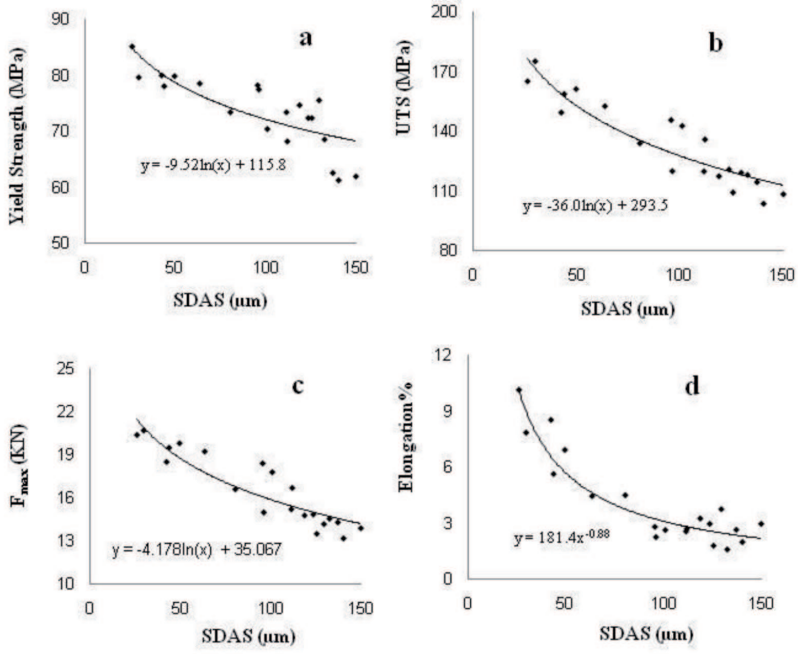

Fig. 3. Variation of yield stress (a), ultimate tensile strength (b), maximum force (c) and elongation percentage (d) with secondary dendrite arm spacing

$$\text{бy} = -9.52\ln(\text{SDAS}) + 115.8 \quad (4)$$

$$\text{UTS} = -36.0\ln(\text{SDAS}) + 293.5 \quad (5)$$

$$F_{max} = -4.178\ln(\text{SDAS}) + 35.067 \quad (6)$$

$$\Delta l = 181.4(\text{SDAS})^{-0.88} \quad (7)$$

Equations 3, 4, 5, 6 and 7 are incorporated in the software as solidification code for prediction of mechanical properties in modeling.

4. Validation of the model

Comparison of the model's predictions with experimental measurements of secondary dendrite arm spacing for A356 alloy is displayed in Fig. 4. The higher consistency of this model with experimental measurement in relative to other models can be easily observed.

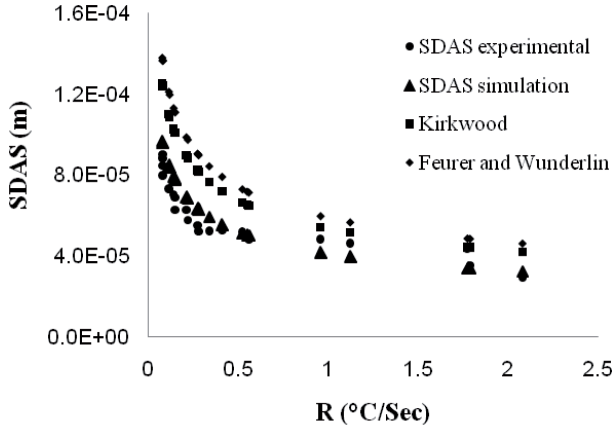

Fig. 4. Comparison of the model's predictions with experimental measurements of secondary dendrite arm spacing for A356 alloy

Figure 5 shows the variations of yield stress, ultimate tensile strength, elongation percentage and F_{max} with cooling rate. It is revealed that predictions of this study are consistent with the experimental measurements of these properties for A356 alloy.

In order to predict the mechanical properties of A356, The UTS distribution and the yield stress distribution in this model are displayed in Figure 6.

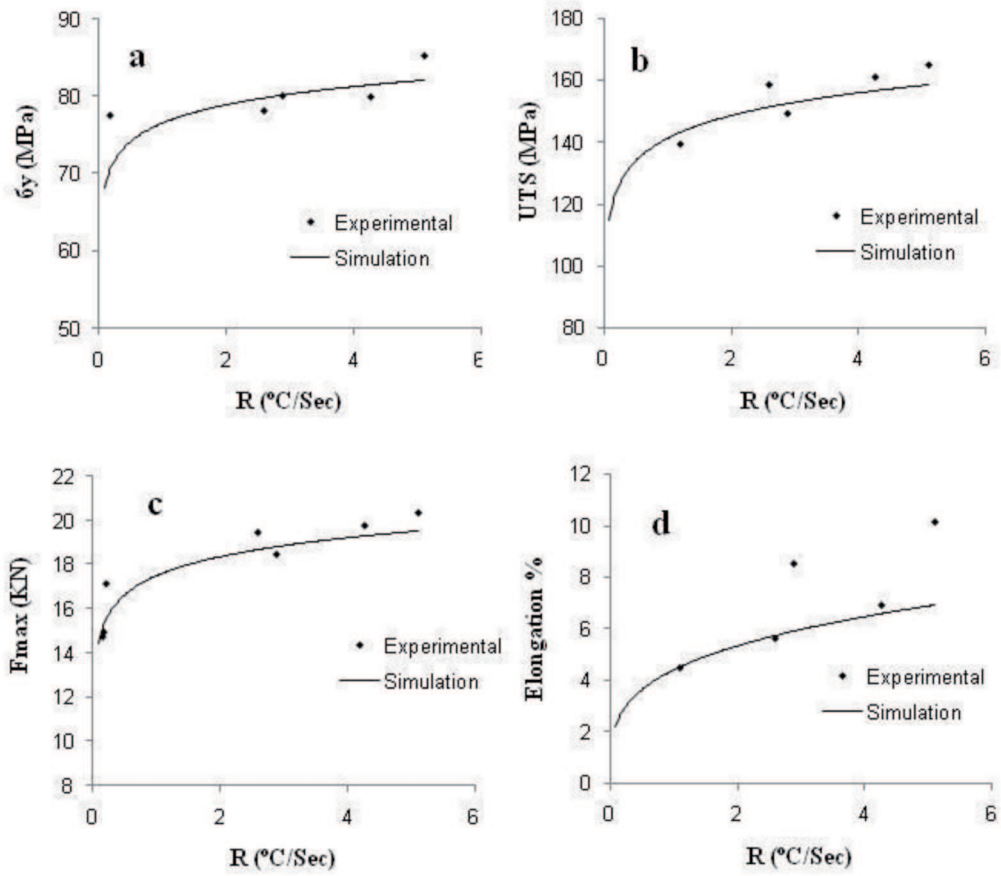

Fig. 5. Variation of yield stress (a), ultimate tensile strength (b), F_{max} (c) and elongation percentage (d) with cooling rate

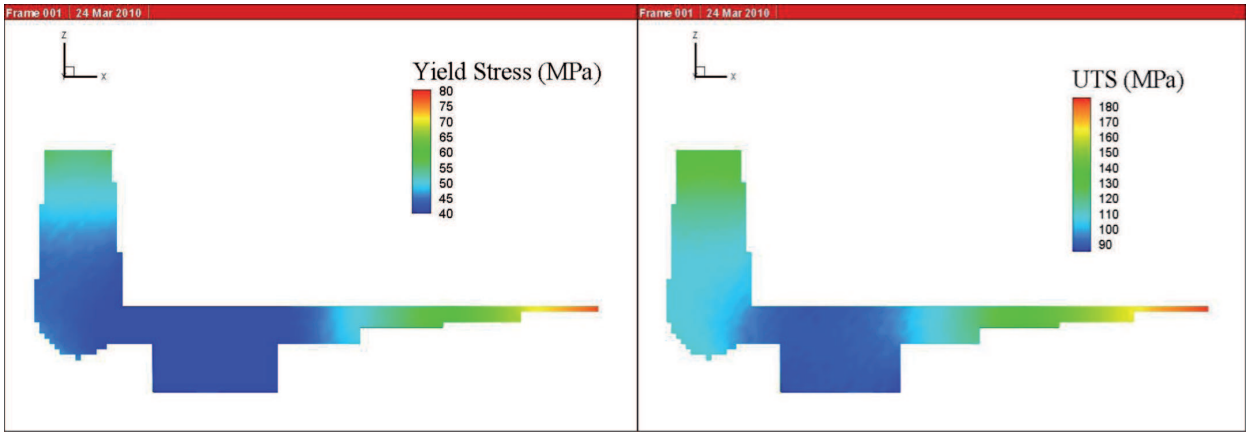

Fig. 6. The UTS distribution (right) and the yield stress distribution (left) in this model

5. Conclusions

1 – Mechanical properties modeling of solidification in A356 alloy was developed in order to predict the yield stress, Ultimate Tensile Strength, F_{max} and elongation.

2 – Analytical equations obtained in this study are incorporated in the post processing step of commercial solidification codes.

3 – Predictions of mechanical properties show excellent agreement with experimental measurements which indicates that the models described in this paper provide a convenient approach to determine the mechanical properties in A356 aluminum alloy.

REFERENCES

[1] S.A. Kori, B.S. Murty, M. Chakraborty, Mater. Sci. Eng. **A 283**, 94-104 (2000).
[2] P.E. Croseley, L.F. Mondolfo, AFS Trans. **74**, 53-64 (1966).
[3] L. Heusler, W. Schneider, J. Light Met. **2**, 17-26 (2002).
[4] A.M. Gokhale, G.R. Patel, Mater. Sci. Eng. **A392**, 184-190 (2005).
[5] X. Jian, H. Xu, T.T. Meek, Q. Han, Mater. Lett. **59**, 190-193 (2005).
[6] S.G. Shabestari, H. Moemeni, J. Mater. Proc. Technol. **153-154**, 193-198 (2004).
[7] Ch.A. Gandin, Iron Inst. Steel Jpn. **40**, 971 (2000).
[8] K.T. Kashyap, S. Murali, K.S.S. Murthy, Mater. Sci. Technol. **9**, 189-203 (1993).
[9] N.L.M. Veldman, A.K. Dahle, D.H. Stjohn, L. Arnberg, Metall. Mater. Trans. **32A**, 147-155 (2001).
[10] S. Gowri, F.H. Samuel, Metall. Mater. Trans. **A 25A**, 437-448 (1994).
[11] Q.G. Wang, C.J. Davidson, J. Mater. Sci. **36**, 739-750 (2001).
[12] Yuhong Zhao1, Hua Hou, Institute of Physics Publishing, Conference Series. **29**, 210-219 (2006).
[13] M.D. Peres, C.A. Siqueira, A. Garcia, Alloys and Compounds. **381**, 168-181 (2004).
[14] Q. Han, S. Viswanathan, Oak Ridge National Laboratory, P.O. Box 2008, Oak Ridge, TN 37831-6083.
[15] Pedro R. Goulart, Jos'e E. Spinelli, Wislei R. Os'orio, Amauri Garcia, Materials Science and Engineering. **A 421**, 245-253 (2006).

Received: 10 February 2011.